ISSN: 2833-9312

Research Article

World Journal of Clinical & Medical Images

Biostatistical and mathematical analysis on liver disease during COVID-19 pandemic

Bin Zhao[1*], Xia Jiang[2]

[1]*School of Science, Hubei University of Technology, Wuhan, Hubei, China.*

[2]*Hospital, Hubei University of Technology, Wuhan, Hubei, China.*

***Corresponding author**

Bin Zhao, School of Science, Hubei University of Technology, Wuhan, Hubei, China.

Submitted: 07 Oct 2022; **Accepted:** 11 Oct 2022; **Published:** 18 Oct 2022

Citation: *Bin Zhao, Xia Jiang, (2022). Biostatistical and mathematical analysis on liver disease during COVID-19 pandemic, World J Clin Med Img, 2022, 1(2), 84-97.*

Abstract

The liver is the body's biggest organ and is involved in metabolic processes. The liver is involved in both metabolism and dehydration. It helps in the detoxification of harmful chemicals as well as the growth of microorganisms. For systemic removal and preservation of organisms and other creatures, the liver is the most essential organ. As a result, liver injury has significant ramifications. Liver disease is regarded as a serious health issue. Overuse of several medicines, which are occasionally prescribed as part of treatment, can cause organ damage. Hepatotoxicity is caused by other chemical agents, such as those employed in labs (thioacetamide, alcohol, etc.) and industry, as well as natural compounds (such as microcystin). Many over-the-counter medicines aren't prescribed to help people with liver disease, and they can actually harm the liver. As a result, plant-based treatments are utilised to treat liver illness. As a result, several human herbal treatments have been evaluated in experimental animal models for antioxidant and hepatoprotective liver function. Acanthus ilicifolius was used as Traditional Chinese medicine (TCM) and Traditional Indian medicine (TIM). The plants showed many clinical properties. Still, the neurological related functions and disorders are not well explored in this plant. Complex interplay of positive and negative emotions orchestrated by intricately associated neuronal circuits, neurotransmitters coupled with endocrinal in- fluence holds responsible for human behavior, considered as the root of human civilization, is currently facing existential crisis during COVID-19 pandemic. In the present study, an attempt was made to identify the interaction between A. ilicifolius natural compounds and Echinacoside as reference compounds were to study the neurotransmitters functions through biomathematical and computational method. Initially, in silico molecular docking was performed to identify the potent natural compounds against neurological disease. The results show among 8 natural compounds, 26.27-Di(nor)- cholest-5,7,23-trien-22-ol, 3-methoxymethoxy, Cholest-5-en-3-ol (3, Beta.)-, carbonochloridate, Cholesterol and Echinacoside exhibited maximum interaction with all the target proteins. Especially, Echinacoside exhibited the maximum interaction with (Serotonin) 5- hydroxytryptamine receptor 2A (-17.077), Sodium-dependent serotonin transporter (-15.810) and (Histamine) Histamine H2 receptor (-17.556). These two neurotransmitters act as a major concern related to the mental disorders and neurological functions. The natural compounds may potent inhibitor for neurological disorders.

Keywords: Liver, Herbs. Neurotransmitters, Acanthus ilicifolius, Echinacoside, In silico

Introduction

The liver is an essential organ that regulates many physiological processes in the body. This contributes to important functions, such as metabolism, excretion, food resistance and energy. The liver is supposed to defend itself from the hazards of medicines and chemicals in addition to performing medicinal functions. The liver plays an important role in many important physiological processes such as glucose homeostasis, essential protein production, lipoprotein and lipid production, bile acid excretion and vitamin accumulation. It is widely reported that foreign substances, hepatotoxins, and chemotherapy impair its function. Damage due to chronic alcohol abuse, bacterial hepatitis, or metabolic disorders. Cellular necrosis, fibrosis, increased tissue oxidation, and reduced tissue glutathione levels are all linked to liver injury. By introducing lipid peroxides and other harmful effects, a vast range of hazardous substances harm liver cells. The most common causes of liver disease are viral infections, medications, toxic chemicals, alcohol abuse, and autoimmune problems. A large number of hepatotoxic chemicals destroy liver cells due to lipid peroxidation and other oxidative damage. One of the most serious health issues is liver disease and steroids, antibiotics and antibiotics are recommended as treatments for liver disease. The treatment has many side effects especially when used for long time. There is a universal method of using traditional herbal methods to treat many liver diseases. Natural herbal remedies have been known to be hepatoprotective agents

that contain a wide variety of chemicals. Herbal medicines have gained popularity and popularity around the world because to their safety in recent years, security and cost. According to the World Health Organization (WHO), about a quarter of the world's population uses traditional or herbal medicine for a variety of ailments, including liver disease. Medicinal herbs have been proven to be effective in treating viral and communicable illnesses in several investigations. Allopathic medication can be used to cure hepatitis and liver damage in clinical trials, but reports of numerous adverse effects, such as immunosuppression, bone loss, and renal failure, led other herbal medicine researchers to believe that it had little impact, but without experiencing it. It is quite successful in the treatment of hepatitis.

Materials and Methods

Herbal medicine dates back to 2100 BC in ancient China's Xia dynasty, This was written for the first time in 600 BC. There are more than 300 preparations in the traditional Indian medical system for treating jaundice and chronic liver disease. The semi -synthetic properties of

these compounds will also be useful in the pharmaceutical sector. The ingredients found in this ingredient provide an excellent therapeutic effect with few side effects and low cost. Antioxidants have also been shown to reduce toxicity. Natural antioxidants are broken down into several compounds as secondary metabolites.

Polyphenols (phenolic acids and flavonoids), terpenoids (carotenoids), and foods containing significant amounts of these chemicals, for example, have an essential role in illness prevention. Plant-derived medicines are utilised in medicine. The current study is based on reported research work on hepatoprotective phytochemicals from different medicinal plants tested for various types of hepatotoxicity [1-17].

Collection and Authentication of Plant

A. ilicifolius leaves were collected from Cuddalore District, Tamil Nadu, India and authenticated by the Botanical Survey of India, Tamil Nadu Agriculture University, Coimbatore, Tamil Nadu, India. (BSI/SC/5/23/09-10/Tech. 306). A voucher specimen of the plant has been deposited at the Herbarium of Botanical Survey of India.

Preparation of the leaf extracts

The fresh leaves of *A. ilicifolius* were washed and shade dried at room temperature (28 ± 2ºC). The dried leaves were powdered by the electrical blender. 25 gms of *A. ilicifolius* leaf powder was used for methanol extraction in the Soxhlet apparatus [18]. The solvent was boiled gently at 64ºC in a heating mantle until the extraction was done. Then the solvent was evaporated using a rotary vacuum evaporator to yield a viscous dark green residue of methanol leaf extracts.

Identification of phytochemicals

The GC-MS of *A. ilicifolius* methanolic leaf extract was identified compounds are 26.27- Di (nor)-cholest-5, 7, 23-trien-22-ol, 3-methoxymethoxy (RT=12.31). 9H –purin-6-amine, N, 9- bis (trimethylsilyl)-8-((trimethylsilyl) oxy) (RT=14.09). Cyano colchicines (RT=6.06). 3Beta- methoxy-5-cholesten-19-oic acid (RT=18.46) [19].

Cholest-5-en-3-ol (3, Beta.)-, carbonochloridate (RT=25.978), Cholesterol (RT=27.518), Cholest-5-en-3-ol (3, Beta.)-, propionate (RT=28.51) and Echinacoside [20]. Infrared spectroscopy identifies the functional group present in the above-listed compounds, the presence of alcohols and phenols in the O-H region at 3389 cm-1.

In silico studies

Preparation of Ligands and standard drug

The hepatoprotective power of the hydrochemical extraction of Aervalanata extract against paracetamol, which induces hepatotoxicity, was discussed. Liver damage can occur with the use of paracetamol up to 3 g / kg. In paracetamol-fed mice, liver enzymes such as ALT, AST, ALP, and serum bilirubin rose substantially ($P < 0.001$) compared to normal controls.

When mice were given Avera lanata extract instead of paracetamol, drug-induced hypersensitivity factors such as liver enzyme ($p<0.01$), and ALT ($p<0.001$) changed significantly ($p<0.01$). Hepatoprotective silymarin (25 mg/kg) given as standard resulted in a substantial decrease in liver enzyme and bilirubin levels ($p<0.001$) when likened to paracetamol.From the above analysis, it can be assumed that the medicinal plant Aervalanata has been shown to be a liver-protecting herb (Manokaran et al., 2008).

The seven major phytochemical compounds considered are: 26.27-Di (nor)-cholest-5, 7, 23-trien-22-ol, 3-methoxymethoxy, 9H –purin-6-amine, N, 9-bis (trimethylsilyl)-8- ((trimethylsilyl) oxy), Cyanocolchicines and 3Beta-methoxy-5-cholesten-19-oic acid. Cholest-5- en-3-ol (3, Beta.)-, carbonochloridate, Cholesterol, Cholest-5-en-3-ol (3, Beta.)-, propionate and Echinacoside structures were retrieved from Protein data bank (PDB) and ISIS Draw 2.3 software (freeware) (http://chemfan.pg.gda.pl/Oprogramowanie/Program/Draw23.exe) was used to design the ligands.

Analogs were changed into MOL files and 3D optimization was done by ChemSketch 3D viewer of ACDLABS 8.0.

The standard drug was used for comparison. Acetylcholine, Dopamine, GABA, Glutamic acid, Norepinephrine, Serotonin, and Histamine were collected from PubChem.

ADME property of active components

Lipinski rule of five is used to check the Adsorption, Distribution, Metabolism, and Excretion (ADME) orally active drug in humans.

This was done by ADME tool. OSIRIS Property Xplorer was used to validate the drug molecule (Active phytochemicals) which has an inhibitory effect on the modeled target protein. Properties such as mutagenicity, irritant, tumorigenic and drug likeliness of the phytochemicals were studied [21, 22].

Collection of Target proteins for HCC

The lists of target proteins for neurotransmitters were collected through a literature survey and structures were retrieved from the Protein Data Bank (PDB) shown in Table 1.

Table 1: List of neurotransmitters receptors

S. No	Gene name	PDB ID	Protein name	Reference
1	Acetylcholine	5CXV	Muscarinic acetylcholine receptor M1	[23,24]
		3UON	Muscarinic acetylcholine receptor M2	
		4U14	Muscarinic acetylcholine receptor M3	
		5AFH	Neuronal acetylcholine receptor subunit alpha-7	
2	Dopamine	6CM4	D2 dopamine receptor	[25]
3	GABA	4MR7	Gamma-aminobutyric acid type B receptor subunit 1	[26]
4	Glutamic acid	2ZNT	Glutamate receptor ionotropic, kainate 1	[27]
5	Norepinephrine	2R4S	Beta2 adrenoceptor	[28]
6	Serotonin	5TUD	5-hydroxytryptamine receptor 2A	[29]
		5I71	Sodium-dependent serotonin transporter	
7	Histamine	3SN6	Histamine H2 receptor	[30]

Molecular Docking of *A. ilicifolius* phytochemicals against HCC target proteins

The structure was minimized using OPLS-2005 force field with Polack-Ribiere Conjugate Gradient (PRCG) algorithm. The Schrodinger Glide program version 2017 has been used for docking. The best 10 poses and corresponding scores have been evaluated using Glide in single precision mode (GlideSP) for each ligand. For each screened ligand, the pose with the lowest Glide SP score has been taken as the input for the Glide calculation in extra precision mode (Glide XP). The docking was carried out with the following non-default settings in Glide SP and Glide XP both [31].

Results and Discussion

The leaves and fruits of Azadirachta indica play a vital function in traditional medicine, and they are a key element of its therapeutic properties. Imbidine, margosic acid, nimbine, and polysaccharides are the active phytochemical components. Medical activities include antiemetic, antineoplastic, emetic, antisyphilitic, emollient, stimulant, aphrodisiac, carminative, antiasthmatic, astringent, antihelminthic, antiseptic, antimalarial and anti-inflammatory. Fresh

Azadirachta indica juice was found to decrease paracetamol-induced lipid peroxidation in one research. It is given orally in a dose of 200 mg/kg with freshly squeezed juice. Orally, a dosage of 2 g/kg paracetamol is given. The decrease in sulfhydryl and group hepatocytes was avoided by drinking freshly squeezed juice. The concentration of liver enzymes in the blood increases after taking paracetamol. Enzyme levels in the blood stay constant when Azadirachta indica is administered.Ashfaq et al. discovered a phytochemical (3-deacetyl-3-cinnamoyl-azadirachtin) that has antibacterial action against the HCV NS3 protease, as well as molecular and mimetic mechanisms that can serve as NS3 / 4A protease inhibitors, in the literature. Gupta and Chaphalkar examined the immunomodulatory and anti-inflammatory properties of A. indica extract in the presence of a range of antibiotics (DPT, hepatitis and rabies). Antimicrobial DPT, HBsAg, and antibiotics showed lower IgG levels, as well as fewer granulocytes, monocytes, and lymphocytes in whole blood, than A. indica. As a consequence, A. indica-containing plants are a strong candidate for commercial vaccines that not only promote, but also sustain, high immune status against HBsAg, DPT, and rabies.

Structure and function of the neurotransmitters by Bio-Mathematical Model

Bombacaceae are medicinal plants that can come from the tropical regions of the Indian subcontinent. Its treatment has been carried over into traditional health systems such as Ayurveda, Siddha and Unani. The protective function of removing methanol from Bombax cepa L flowers tested against isoniazid and rifampicin produced hepatotoxicity and high levels of albino Wistar. Hepatotoxicity in mice was associated with two antituberculous drugs, isoniazid and rifampicin for 10-21 days intraperitoneally in mice. Three doses of Bombax ceiba L. (150, 300 and 450 mg / kg of active ingredient) were administered to study the protective function of the liver. From the normal range, there was a substantial increase in AST, ALT, ALP, total bilirubin, and a significant decrease in total isoniazid protein and rifampicin levels. Taking different drugs of Bombax Cipa-L can alter the levels of enzymes in the blood. Obviously this plant reduced TBARS levels and increased GSH levels at all doses compared to normal control. The liver tissue of animals treated with Bombax ceiba L. protects against liver damage caused by isoniazid and rifampicin. In addition to the hepatotoxicity of this plant, it is also widely used for its anti-inflammatory, antihypertensive, vascular and antioxidant activity.

Calotropis gigantean ethanol fruit was discovered for its hepatoprotective properties. Ethanol produces liver damage. High levels of AST, ALT, ALP and LPO, as well as low levels of vitamin C, indicate significant liver damage in toxic animals. Treatment before weight gain of 250 to 500 mg / kg of Calotropis gigantean tissue released reduced levels of enzyme markers, lipid peroxidation, and an increase in blood vitamin C. The pharmacological

effects of the extract may be due to its antioxidant ability to prevent lipid peroxidation and prevent damage to vitamin C.

Citrus retinol essential oil has been listed for its hepatoprotective properties. Is isoniazid (50 g / kg, po. For 30 days) developed hepatotoxicity. Essential oils (200 mg / kg, p.o.) were administered every 24 hours for 30 days, while a standard received Liv52. At the end of the study, the red blood cell content was estimated. The treated isoniazid showed only a significant increase in ALT, AST and bilirubin and a significant reduction in total protein compared to normal (non-isoniazid-associated) control animals. Animals treated with cross-linked citrus and Liv52 essential oils showed significant reductions in all studies. In other words, the above results suggest that the citrus lattice has a potent hepatoprotective function against liver damage caused by isoniazid.

Hepatotoxic effects of Cissaampelos pareira ethanolic root extract at different dosages of 100 mg/kg, 100 mg/kg, 100 mg/kg, and ccl4 in rats were discovered. SGOT, SGPT, ALP, and bilirubin levels were measured to evaluate liver function. Hepatotoxicity can be induced in this case by mixing ccl4 with olive oil (weight 2 ml/kg, i.p.). The hepatotoxicity group had higher levels of biosystems such SGOT, SGPT, ALP, and bilirubin. The ethanol extraction of Cissaampelos pareira root has a strong protective effect, lowering the biochemical potential to near-normal levels.Historical research shows control of root extract in ccl4, indicating safety in the liver.

The therapeutic effect of the removal of toxic fruit and sharp seeds of Embeliatsjeriam- cottam and liver damage with isoniazid in mice was investigated. One treatment with isoniazid (50 g / kg for 30 days) showed an increase in ALT, AST, bilirubin and significant reduction in total protein compared to normal control. An animal treated with an alcoholic drink showed what showed severe side effects with all the ingredients of the chemical. In vivo peroxidation studies showed that mice from the isoniazid treatment group demonstrated this significant increase in malondialdehyde (MDA) compared to the high control dose. The use of alcohol and intoxicants reduces MDA levels. There was a decrease in GSH levels, SOD activity and treatment with CAT and isoniazidone over a normal control. Levels of GSH, SOD and CAT increased significantly in alcohol and single drug extraction. The subjects' liver biopsy studies showed normal hepatocytes and normal liver morphology. Liver of killer mice with isoniazid Cavity, sinus congestion, mild inflammation and damage of hepatocytes with central necrosis are present. Both alcohol and Embeliatsjeriam-cottam alcohol extracts can reduce hepatotoxicity caused by isoniazid.

Orthosiphon is an important ingredient commonly used in Malaysia to treat various types of liver diseases. Hepatotoxicity and hepatotoxicity of thioacetamide were studied with ethanol supplementation in Sprague Dawley rats. A maximum of 40 samples were taken for the experimental design. The five groups of adult rats were group 1 (control), group 2 thioacetamide as an active control (one hepatotoxic group), and group 3 silymarin as a known medicine (hepatoprotective group) (each comprising eight animals). , as well as tiny and micro dosages, belong to groups 4 and 5. (single treatment). All rats were killed after two months of treatment. When compared to normal animals, the hepatotoxic group showed a substantial rise in HCC (ALT, AST, ALP, and bilirubin) and malondialdehyde (MDA) levels, as well as a significant decrease in protein and albumin levels. The high therapeutic effect and ethanol extract of Orthosiphon Stamineus (200 mg / kg) alters liver function enzymes in high doses to be beneficial. These studies indicate that Orthosiphon stamineus is an important Ayurvedic plant with hepatotoxic effects on thioacetamide-induced hepatotoxicity in rats.

The hepatoprotective and antioxidant activity of the methanolic extract of Phyllanthus polyphilus against paracetamol-induced hepatotoxicity was discussed. Plant production showed strong hepatoprotective effect and antioxidant activity against paracetamol leading to hepatotoxicity and mice. Liver enzyme and lipid peroxidase (LP) were all elevated in animals given 750 mg/kg paracetamol. TC and total protein (TP) are reduced, as are superoxide dismutase (SOD), catalase, glutathione peroxidase (GPx), and glutathione S-transferase (GST). Different therapeutic medicines (200 and 300 mg / kg, p.) were used. that Phyllanthus polyphyllus has strong liver-in-protective and antioxidant properties.

The protective effect of ethanol extracted from Pyrenacanthastaudtii and carbon tetrachloride (CCl4) was induced by hepatotoxicity in rats in experimental studies. Sixteen Wistar rats weighing 100-170 g were divided into four groups, divided into groups I, II, III and IV. The second, third and fourth doses of 5l / kg of CCl4 weight were injected intraperitoneally while 5ml / kg of crude oil was injected in the normal control. After 48 hours, Pyrenacanthastaudtii ethanol of groups III and IV (750 mg / kg and weight 1500 mg / kg) was administered, respectively. The mice were then removed 5 days later. Based on the research on drivers, it was shown that two ethanol (750 mg / kg and 1500 mg / kg weight) reduced the levels of liver enzymes which increased significantly with the treatment dose ccl4. CCl4 animals had increased bilirubin levels in mice compared to mice. But two levels of ethanol significantly altered bilirubin levels depending on the type. The release of Pyrenacanthastaudtii has hepatoprotective effects against hepatotoxicity and damage caused by CCl due to the presence of flavonoids and other bioactive substances.

Tecomella undulate

Known for its methanol derivatives of the famous herb, Tecomella leaf damage against alcohol and acetaminophen caused liver damage and excessive albino. Levels of blood enzymes such as AST, ALT, ALP, GGT (gamma-glutamyl transpeptidase) and total bilirubin in the blood associated with the activity of LPO (lipid peroxidase), SOD (superoxide dismutase), CAT catalase), GSH (reductase) GPx A glutathione peroxidase in the liver is treated in this way. Historical changes in liver function were also compared with related controls. The enzymatic component of hepatic oxidative stress markers (SOD, CAT, GSH and GPx) increased significantly ($p < 0.001$) and LPO was significantly reduced in alcohol consumption by 30% by paracetamol. In 30 percent alcohol and paracetamol mice, oral therapy with Tecomella undulate (100 mg / kg, 200 mg / kg, btBt / day) altered all serological and hepatic alterations. The medication silymarin

(25 mg / kg bw / day) was also used to compare biochemical data. These findings show that the presence of flavonoids, quinones, and other antioxidants in ticumilla wafer leaves may give liver protection.

In rats, the hepatotoxicity of Ziziphus mauritiana leaf extract was reported to produce hepatotoxicity. Wistar Albino dosages of 100-120 g were given in one of six single doses and the animals were treated for six weeks. Prolonged alcohol intake (40 percent v/v, 1 ml / 100 g), increased for six weeks (p0.05), and liver enzyme and total bilirubin levels might cause hepatotoxicity (TB). In comparison to normal controls, the levels of catalase, glutathione peroxidase, glutathione reductase, and superoxide dismutase all decreased significantly (p0.05).Meanwhile, therapy with Ziziphus mauritiana 200 mg/kg or silymarin 100 mg/kg resulted in near-normal ALT, AST, ALP, and TB levels that were statistically significant (p0.05). When Ziziphus mauritiana was given instead of alcohol, excellent antioxidant measures including catalase, glutathione peroxidase, glutathione reductase, and superoxide dismutase were significantly increased. Cell death, fat burning, and other histopathological features of alcoholic liver suggest liver injury. Rehydration treatment with Ziziphus Mauritania or silymarin reduces tissue damage and cell death caused by persistent drinking.Ziziphusmauritiana's protective role is to block antioxidant substances such tannins, saponins, and phenolic compounds, among others.

Typical neuron mathematical equation

A typical neuron is generally classified into three parts namely cell body, dendrites, and axon [32]. The cell body contains the nucleus and associated intracellular structures whereas, dendrites are the extension of the cell body. Axon carries information from the cell body to other cells (receiving cell). Dendrites and axons, both extensions of the cell body, are also referred to as processes.

For the typical neuron, a simple model is as follows:

$$N = K(C + D + A) \qquad (2.1)$$

where N is the neuron; C is the Cell body; D is the Dendrites; A is the Axon; K is the diffusion coefficient. Factors that relate to the K, are the neuron weight, degree of ionization, neuron space configuration, and the condition that whether it combined with the three distinct parts.

Cell body

Cell body assimilates the synaptic input and transmits the determined message to another cell by the axon. It was found to be responsible for the diversity of biochemical process such as transforming glucose into high-energy compounds to other parts of the neuron, highly active proteins serve as chemical messengers between cells are manufactured and packaged and specialized organelles perform the cell's function. Sheng Chen [33] proposed a mathematical theory for hormonal functions in the cell body were as follows:

where f_i is one hormonal function of the cell body, and f_i is made up of three main parts:

f_i(C1,C2 , S1(t)), f_2 (C1,C2 , S2 (t)).

Dendrites

Dendrites expand its sensitive receptive surface to the surrounding nervous tissue, reflects the function of the cell and the functional properties can be predicted from the pattern of dendritic branching. The thin branching and treelike forms increase the chance for synapticconnections in the brain [34]. Dendrites in the many neurons present with a special form of synaptic connection called dendritic spines. They are small (1-2 µm), a thorn-like protuberance from the dendrite and are the major anatomical feature of neurons in the human nervous system. According to the definition of dendritic spines, suppose that the dendritic spines are

$e = x + y$. If for any $x(0)$, y (0) satisfy the condition

$\lim_{t\to\infty}\|e\| = \lim_{t\to\infty}\|x(t)+y(t)\| = 0$, then we say

that system (2.1) and system (2.2) achieve modifiable structures. On the basis of adaptive control methods, we can give the following equations and the stability of neural networks with the dendritic structure:

$$\begin{cases} u_1(t) = -D_t^{\beta_1}x_1 - D_t^{\alpha_1}x_1 - (\hat{a}(y_2 - y_1) + y_4) + \hat{a}(x_2 - x_1) + x_4 - k_1e_1 \\ u_2(t) = -D_t^{\beta_2}x_2 - D_t^{\alpha_2}x_2 - (\hat{h}(y_1 - y_1y_3 + \hat{c}y_2) + \hat{h}x_1 - x_1x_3 + \hat{c}x_2 - k_2e_2 \\ u_3(t) = -D_t^{\beta_3}x_2 - D_t^{\alpha_3}x_2 - (y_1y_2 - \hat{b}y_3) + x_1x_2 - \hat{b}x_3 - k_3e_3 \\ u_4(t) = -D_t^{\beta_4}x_2 - D_t^{\alpha_4}x_2 - (y_2y_3 + \hat{r}y_4) + x_2x_3 + \hat{r}x_4 - k_4e_4 \end{cases} \qquad (2.3)$$

where $e_1 = x_1 + y_1$, $e_2 = x_2 + y_2$, $e_3 = x_3 + y_3$,$e_4 = x_4 + y_4$, $k_i > 0$, (i = 1, 2, 3, 4). If t $\to\infty$, then

$\|e\|\to 0$,and system (1) and system (2) achieve modifiable structures indicating the possibility that the pineal gland, a primary source of dendrites.

If we put (3) and system (1) to the system (2), then the following error equations can be obtained between the groups for some fractional differential equations and the central nervous system:

$$\begin{cases} D_t^{\beta_1}e_1 = -e_a(x_2 - x_1) - k_1e_1 \\ D_t^{\beta_2}e_2 = -e_dx_1 - e_cx_2 - k_2e_2 \\ D_t^{\beta_3}e_3 = e_bx_3 - k_3e_3 \\ D_t^{\beta_4}e_4 = -e_rx_4 - k_4e_4 \end{cases} \qquad (2.4)$$

where $e_a = a - \hat{a}$, $e_b = b - \hat{b}$, $e_c = c - \hat{c}$, $e_h = h - \hat{h}$, $e_r = r - \hat{r}$ are the parameter estimation errors.

Next, according to (4), we design the adaptive update law for each parameter estimation error:

$$\begin{cases} D_t^{\beta_5}e_a = (x_2 - x_1)e_1 \\ D_t^{\beta_6}e_b = -x_3e_3 \\ D_t^{\beta_7}e_c = x_2e_2 \\ D_t^{\beta_8}e_h = x_1e_2 \\ D_t^{\beta_9}e_r = x_4e_4 \end{cases} \qquad (2.5)$$

where $0 < \beta_i < 1$,(i = 5, 6, 7,8,9), and (5) are obtained by eliminating the dendritic potentials from the underlying compartmental model or cable equations [35].

Axon

Axon is the excitable membrane that extends to the region of synaptic contact and generates or propagate the action potential. Generally, cells contain one axon but there may be off branches or collaterals to transmit the action potential to the brain. The distinctive length of the axon is the action potential and there occurs a Turing-like instability condition as a precursor for pattern formation in a spatially organized network.

According to $e_a = a - \hat{a}, e_b = b - \hat{b}, e_c = c - \hat{c}, e_h = h - \hat{h}, e_r = r - \hat{r}$ and (5), we can get the parameters of the adaptive control law:

$$\begin{cases} D_t^{\beta_5}\hat{a} = (x_1 - x_2)e_1 \\ D_t^{\beta_6}\hat{b} = x_3 e_3 \\ D_t^{\beta_7}\hat{c} = -x_2 e_2 \\ D_t^{\beta_8}\hat{h} = -x_1 e_2 \\ D_t^{\beta_9}\hat{r} = -x_4 e_4 \end{cases} \tag{2.6}$$

According to (4) and (5), we get the total error of the system:

$$D_t^{\beta} E = AE \tag{2.7}$$

where $D_t^{\beta} E = (D_t^{\beta_1} e_1, D_t^{\beta_2} e_2, D_t^{\beta_3} e_3, D_t^{\beta_4} e_4, D_t^{\beta_5} e_a, D_t^{\beta_6} e_b, D_t^{\beta_7} e_c, D_t^{\beta_8} e_h, D_t^{\beta_9} e_r)^{\mathrm{T}}$,

$E = (e_1, e_2, e_3, e_4, e_a, e_b, e_c, e_h, e_r)^{\mathrm{T}}, 0 < \beta_i < 1, (i = 1, \mathrm{L}, 9)$.

Then we consider Eq. (2.7), and expand the formula, we obtain:

$$D_t^{\beta}\begin{pmatrix} e_1 \\ e_2 \\ e_3 \\ e_4 \\ e_a \\ e_b \\ e_c \\ e_d \\ e_r \end{pmatrix} = AE = \begin{pmatrix} -k_1 & 0 & 0 & 0 & -(x_2 - x_1) & 0 & 0 & 0 & 0 \\ 0 & -k_2 & 0 & 0 & 0 & 0 & -x_2 & -x_1 & 0 \\ 0 & 0 & -k_3 & 0 & 0 & x_3 & 0 & 0 & 0 \\ 0 & 0 & 0 & -k_4 & 0 & 0 & 0 & 0 & -x_4 \\ x_2 - x_1 & 0 & 0 & 0 & 0 & 0 & 0 & 0 & 0 \\ 0 & 0 & -x_3 & 0 & 0 & 0 & 0 & 0 & 0 \\ 0 & x_2 & 0 & 0 & 0 & 0 & 0 & 0 & 0 \\ 0 & x_1 & 0 & 0 & 0 & 0 & 0 & 0 & 0 \\ 0 & 0 & 0 & x_4 & 0 & 0 & 0 & 0 & 0 \end{pmatrix}\begin{pmatrix} e_1 \\ e_2 \\ e_3 \\ e_4 \\ e_a \\ e_b \\ e_c \\ e_d \\ e_r \end{pmatrix}$$

Setting $P = E_9$. Then we obtain the following result:

$$\begin{aligned} & AP + PA^T \\ & = A + A^T = -Q \\ & = \begin{pmatrix} -2k_1 & 0 & 0 & 0 & 0 & 0 & 0 & 0 & 0 \\ 0 & -2k_2 & 0 & 0 & 0 & 0 & 0 & 0 & 0 \\ 0 & 0 & -2k_3 & 0 & 0 & 0 & 0 & 0 & 0 \\ 0 & 0 & 0 & -2k_4 & 0 & 0 & 0 & 0 & 0 \\ 0 & 0 & 0 & 0 & 0 & 0 & 0 & 0 & 0 \\ 0 & 0 & 0 & 0 & 0 & 0 & 0 & 0 & 0 \\ 0 & 0 & 0 & 0 & 0 & 0 & 0 & 0 & 0 \\ 0 & 0 & 0 & 0 & 0 & 0 & 0 & 0 & 0 \\ 0 & 0 & 0 & 0 & 0 & 0 & 0 & 0 & 0 \end{pmatrix} \end{aligned} \tag{2.8}$$

where $k_i > 0, (i = 1, 2, 3, 4), Q = diag(2k_1, 2k_2, 2k_3, 2k_4, 0, 0, 0, 0, 0)$.

It is easy to see that $Q = diag\ (2k_1, 2k_2, 2k_3, 2k_4, 0, 0, 0, 0, 0)$ is a semi-positive definite matrix. Then, the state variable of (7) $E = (e_1, e_2, e_3, e_4, e_a, e_b, e_c, e_h, e_r)^T$ is asymptotically stable, that is, $e_1, e_2, e_3, e_4, e_a, e_b, e_c, e_h, e_r$ approach zero asymptotically with time. Therefore, we achieve the neuronal functions in the endoplasmic reticulum by a number of the adap-

tive robust set of fractional differential equations anti-synchronization indicating how the dispersion relation depends on the spatial distribution of the axon-dendritic weights with respect to both network and dendritic coordinates [36]. These primary afferent axons come in different diameters ancan be divided into different groups based on their size. Here, in order of decreasing size, are the different nerve fiber groups: A-alpha (13-20 μm), A-beta (6-12 μm), A-delta (1-5μm) and C-nerve fibers(.2-1.5μm). A-alpha, A-beta, and A-delta nerve fibers are insulated with myelin. C-nerve fibers are unmyelinated. The thickness of the nerve fiber is correlated to the speed with which information travels in it - the thicker the nerve fiber, the faster information travels in it.

The model is described by a hyperbolic system of equations

$$\varepsilon(\partial_t + v_i\partial_x)p_i = \sum_{j=1}^{n} k_{ij}p_j, \quad 0 < x < \infty, \ t > 0, \ 1 \le i \le n,$$

where $k_{ij} \ge 0$ if $i \ne j$, $\sum_{j=1}^{n} k_{ij} = 0$ and $0 < \varepsilon = 1$. Here pi (x,t) is the thickness of the nerve fiber

in one of n nerve fiber groups, and x is the size of the nerve fiber. Setting

$$p_m(x,t) = \lambda_m Q_m\left(\frac{x - vt}{\sqrt{\varepsilon}}, \ t\right),$$

where λ_m is determined by the boundary conditions at $x = 0$ and v is a weighted average of the velocities v_i (v_i can be positive or negative). It is easy to prove that

$$Q_m(s, \ t) \to Q(s, \ t) \quad \text{as} \ \varepsilon \to 0$$

where $Q(s, t)$ is the bounded solution [37]

Overall, Cell body, dendrites, and axon are the three main parts of a neuron. We first consider the existence of positive solutions to parabolic nonlinear genetic equations of the form

where $a(b(u),\nabla u) := f(b(u))\nabla c^*[\nabla(u+V)]$ The dendrite receives the signal from other neurons; then the signal is computed at the synapse and transmitted to the cell body.

And c□ represents the Legendre transform of a function $c:\ ^{d} \to [0,\infty)$ that is

$$c^*(z) = \sup_{x \in R^d}\{< x, z > -c(x)\}$$

for $z \in R^d$ Here, the bounded domain of R^d is Ω including dendrites, cell body with a nucleus, axon; the outward unit normal to $\partial\Omega$ is ν . $b : R \to R$ is a monotone non-decreasing function;

$V : \bar{\Omega} \to R$ is a potential function; $c : Rd \to [0, \infty)$ is a convex function; f is a non-negative real-valued function, and $u^0 : \Omega \to R$ is a measurable function.

The rest is $u : [0,\infty) \times \Omega \to R$, $u = u(t,x)$

If the signal into the cell body exceeds the holding threshold, the cell will fire and send the signal down to other neurons through axon [38].

Function and Transportation of Neurotransmitters

Neurotransmitters are the signaling molecules in neurons that play a vital role in transmitting neural signals through specific receptors, cytomembranes, and postsynaptic membranes. The end of axons of nerve cell secrete neurotransmitters (chemical agents), diffuse and transmit a signal to adjoining cells like muscle cells, neurons, and glands across the synaptic gap by altering its electrical state.

$F : [0,\infty) \to R$, where $F' = b^{-1}$ 。

$\rho := b(u)$, $\rho_0 := b(u_0)$, $f(x) = \max(x, 0)$

Suppose that the neurotransmitters signals function

$$\begin{cases} \dfrac{\partial \rho}{\partial t} = \operatorname{div}(\rho U_\rho) = 0 & (0,\infty) \times \Omega \\ \rho(t = 0) = \rho_0 & \Omega \\ \rho U_\rho \cdot v = 0 & (0,\infty) \times \partial\Omega \end{cases} \qquad (3.1)$$

where $U_\rho := -\nabla c^*\left[\nabla(F'(\rho) + V)\right]$, $\rho_0 :$

$\Omega \to [0,\infty)$, $\rho : [0,\infty) \times \Omega -$

represents the transportation of neural signals by the time t ($t \in [0,\infty)$) and position x. The summation of extracellular neurotransmitter concentration is

$$E(\rho(t)) := \int_\Omega \left[F(\rho(t,x)) + \rho(t,x)V(x)\right]dx.$$

Through the above equations (10) and (11), we can find out that methionine enkephalin (ME), leucine enkephalin (LE), dopamine (DA) are able to diffuse freely into both 1-palmitoyl-2-oleoyl-sn-glycero-3-phosphocholine and 1-palmitoyl-2-oleoyl-sn-glycero-3- phosphoethanolamine membranes and are guided by the aromatic residues Tyr and Phe. Only a limited number of these neurotransmitters are allowed to penetrate into the membrane, which suggests an intrinsic mechanism by which the membrane is protected from being destroyed by excessive inserted neurotransmitters [39].

Transportation of GABA

GABA, a universal nonprotein amino acid, and functions variedly in different organisms (plants, fungi, and bacteria) and mammalian tissues. It acts as an inhibitory neurotransmitter and helps the neurons to recover from the worry, anxiety, and fretfulness [40].

The corresponding system of equations reduces to

$$\frac{\partial \rho}{\partial t} = \Delta\rho + div(\rho\nabla V) \qquad (32)$$

The major predictions from the above equations are as follows: (1) Uptake of GABA is totally sodium-dependent. (2) Although plots of 1/v versus 1/[Na]2 are nonlinear, the coupling ratio for transport (Na/GABA) is 2. (3) For transport to take place, the

order of combination with a carrier must be Na, Na, GABA. (4) Maximal velocity will occur only at infinite Na and GABA concentrations. (5) There is a sigmoidal relationship between apparent maximal velocity (Va) and [Na]. (6) Kt, the [GABA] that gives a velocity equal to Va/2, rises and then falls as [Na] is increased from zero, passing through a maximum at 33.52 mM [Na]. (7) The relationship between initial velocity and [Na] is sigmoidal. (8) Jm, the rate of uptake with infinite [Na], is hyperbolically related to [GABA]; Jm approaches Vmax as [GABA] becomes very large. (9) KNa, the [Na] giving a velocity equal to Jm/2, declines rapidly from 10−7M to 10−5M GABA, but is essentially constant at 10−4M and above. (10) One GABA molecule is translocated per carrier molecule.

Transportation of Serotonin

Kogofsky [41] and other contributors cited that serotonin was one of the major neurotransmitters responsible for many biological processes like appetite, mood disorders, sleep, digestion, depression and generalized well-being.

The corresponding system of equations reduces to

$$\frac{\partial \rho}{\partial t} = \Delta \rho^m$$

$$\left(V = 0, c(z) = \frac{|z|^2}{2}, \quad F(x) = \frac{x^m}{m-1} \quad 1 \neq m \geq 1 - \frac{1}{d} \right). \tag{33}$$

The above equations of serotonin transporter provide a novel genetic and behavioral primate model to study the molecular, neurodevelopmental, and psychopharmacological mechanisms that underlie genetic variation-associated complex behaviors, with specific implications for the understanding of normal and abnormal serotonin actions and the development of personalized pharmacological treatments for psychiatric disorders.

Transportation of Acetylcholine

Acetylcholine was found mostly in neuromuscular junctions and are catalyzed by the acetylcholinesterase enzyme. It is responsible for learning, voluntary movement, sleep and memory and too much of it lead to depression and dementia in case of low level in the hippocampus region [42].

The corresponding system of equations reduces to

$$\frac{\partial \rho}{\partial t} = div\left(\left| \Delta \rho^{\frac{1}{p-1}} \right|^{p-2} \Delta \rho^{\frac{1}{p-1}} \right)$$

$$\left(V = 0, c(z) := \frac{|z|^q}{q}, \frac{1}{p} + \frac{1}{q} = 1 \qquad F(x) = \frac{1}{p-1} x \ln x \qquad p > 1 \right). \tag{34}$$

It is easy to see that the first intron of the ChAT gene encompasses the open reading frame encoding another protein, vesicular acetylcholine transporter (VAChT), which is responsible for the transportation of acetylcholine from the cytoplasm into the synaptic vesicles.

Transportation of Dopamine

Dopamine the inhibitory and excitatory neurotransmitter play the main role in the regulation of reward circuitry and pleasure centers and a dynamic brain chemical for memory and motor skills [43].

The corresponding system of equations reduces to

$$\frac{\partial \rho}{\partial t} = div\left(\left| \Delta \rho \right|^{p-2} \Delta \rho \right)$$

$$\left(V = 0, c(z) := \frac{|z|^q}{q}, \frac{1}{p} + \frac{1}{q}, \quad F(x) = \frac{x^m}{m(m-1)}, \quad m := \frac{2p-3}{p-1}, \quad p \geq \frac{2d+1}{d+1} \right). \tag{35}$$

The major predictions from the above equations involving the effects of dopamine transporter(DAT) overexpression in MN-9D cells on the transportation of dopamine(DA) are as follows: some individuals may be simultaneously more responsive to the effects of environmental adversity and enrichment (i.e., differential susceptibility).

Transportation of Epinephrine

Epinephrine, otherwise called as adrenaline, a hormone responsible for its metabolism. It plays a key role in mental focus, attention, arousal, cognition, inhibits insulin excretion and elevates the number of fatty acids in the blood [44].

The corresponding system of equations reduces to

$$\frac{\partial \rho}{\partial t} = div\left(\left| \Delta \rho^n \right|^{p-2} \Delta \rho^n \right)$$

$$\left(V = 0, \; c(z) := \frac{|z|^q}{q}, \frac{1}{p} + \frac{1}{q}, \quad F(x) = \frac{n x^m}{m(m-1)}, \right.$$

$$\left. m := n + \frac{p-2}{p-1}, \frac{1}{p-1} \neq n \geq \frac{d-(p-1)}{d(p-1)} \right). \tag{36}$$

In the above equations, we established a dynamic mathematical model for detection of diabetes in blood with the help of parameters as epinephrine. In addition to this, we also incorporated a new parameter in the existing model i.e. beta cells which has a great impact on the
insulin.

Transportation of Glutamate

The exciting glutamate neurotransmitter required for memory and learning. Low level of glutamate results in poor brain activity and tiredness and high-level cause death to the neurons in the brain [45].

The corresponding system of equations reduces

$$\begin{cases} \dfrac{\partial \rho^h}{\partial t} = div\{\rho^h \nabla c^* \left[\nabla \left(F'(\rho^h) \right) \right]\} + A(h) & (0, \infty) \times \Omega \\ \rho^h(t=0) = \rho_0 & \Omega \end{cases} \tag{37}$$

The above equations of glutamate transporters tell us that the control of glutamate concentrations is critical to the normal functioning of the central nervous system, and how glutamate transporters regulate glutamate concentrations to maintain dynamic signaling mechanisms between neurons.

Transportation of Histamine

Histamine plays a major role in allergic reactions, affect emotions and behavior, control the sleep-wake cycle and promote the release of epinephrine and norepinephrine.

$$\sum_{i=1}^{T/h}\int_{t_{i-1}}^{t_i}\int_{\Omega}\frac{\rho_i^h(x)-\rho_{i-1}^h(x)}{h}\xi(t,x)dxdt=\frac{1}{h}\int_0^T\int_{\Omega}\rho^h(t,x)\xi(t,x)dxdt$$
$$-\frac{1}{h}\sum_{i=2}^{T/h}\int_{t_{i-1}}^{t_i}\int_{\Omega}\rho^h(\tau-h,x)\xi(\tau,x)dxd\tau$$
$$-\frac{1}{h}\int_0^T\int_{\Omega}\rho_0(x)\xi(t,x)dxdt \quad (38)$$

We use $\tau=t+h$ instead of the above expression to get

$$\sum_{i=1}^{T/h}\int_{t_{i-1}}^{t_i}\int_{\Omega}\frac{\rho_i^h(x)-\rho_{i-1}^h(x)}{h}\xi(t,x)dxdt=\frac{1}{h}\int_0^T\int_{\Omega}\rho^h(t,x)\xi(t,x)dxdt$$
$$-\frac{1}{h}\int_0^{T-h}\rho^h(t,x)\xi(t,x)dxdt$$
$$-\frac{1}{h}\int_0^h\int_{\Omega}\rho_0(x)\xi(t,x)dxdt$$
$$=-\int_0^T\int_{\Omega}\rho^h(t,x)\partial_t^h\xi(t,x)dxdt$$
$$+\frac{1}{h}\int_{T-h}^T\rho^h(t,x)\xi(t+h,x)$$
$$-\frac{1}{h}\int_0^h\int_{\Omega}\rho_0(x)\xi(t,x)dtdx \quad (39)$$

2.2. In silico molecular docking towards Neurodegenerative Disorders

ADME/Tox filtering rules such as molecular weight, polar surface area, logP or number of rotatable bonds shown in Table 2. Target proteins were retrieved from PDB (Protein Data Bank). The Schrodinger Glide program version 2017 has been used for docking [46-48] shown

in Table 3. The hydrogen interactions between ligands and target proteins are shown in Figure 1 (A, B, C).

Table 2. ADME properties of active phytochemical components

S. No	Ligand	$LogK_a^{HSA}$	Physical-chemical properties			Log P
			Molecula Weight	H2 donors	H2 acceptors	
1	26.27-Di(nor)-cholest-5,7,23-trien-22-ol, 3-methoxymethoxy	1.118	414.627	1,000	5,100	5.785
2	9H –purin-6-amine, N,9-bis(trimethylsilyl)-8-((trimethylsilyl) oxy)	0.998	367.672	1,000	4,000	5.157
3	Cyanocolchicines	-0.576	424.452	000	9,500	1.902
4	3Beta-methoxy-5-cholesten-19-oic acid	1.414	430.670	1,000	3,700	7.011
5	Cholest-5-en-3-ol (3, Beta.)-, carbonochloridate,	1.809	383.66	1	1.7	6.916
6	Cholesterol	1.843	386.66	1	1.7	6.999
7	Cholest-5-en-3-ol (3, Beta.)-, propionate	2.371	442.724	0	2	8.418
8	Echinacoside	-2.248	786.736	12	28.8	-3.648

Table 3. Identification of new chemical entities through in-silico drug design method

S. No	Ligand	Target Protein	Docking Score	H-H interaction
1	26.27-Di (nor)-cholest-5, 7, 23-trien-22-ol, 3-methoxymethoxy	Muscarinic acetylcholine receptor M1	-9.274	LYS 57
		Muscarinic acetylcholine receptor M2	-5.268	-
		Muscarinic acetylcholine receptor M3	-9.974	ASN 507
		Neuronal acetylcholine receptor subunit alpha-7	-10.122	-
		D2 dopamine receptor	-6.390	ALA379
		Gamma-aminobutyric acid type B receptor subunit 1	-6.390	ALA379
		Glutamate receptor ionotropic, kainate 1	-7.868	-
		Beta2 adrenoceptor	-7.285	ASN 312
		5-hydroxytryptamine receptor 2A	-7.213	LEU 209, ASP 135
		Sodium-dependent serotonin transporter	-7.499	TYR 175, GLU 493
		Histamine H2 receptor	-6.115	ASN 293, TYR 316
2	9H –purin-6-amine, N,9-bis(trimethylsilyl)-8-((trimethylsilyl)oxy)	Muscarinic acetylcholine receptor M1	-5.812	LYS 57
		Muscarinic acetylcholine receptor M2	-4.498	-
		Muscarinic acetylcholine receptor M3	-6.630	-
		Neuronal acetylcholine receptor subunit alpha-7	-3.911	-
		D2 dopamine receptor	-2.938	-
		Gamma-aminobutyric acid type B receptor subunit 1	-2.939	-

		Glutamate receptor ionotropic, kainate 1	-3.875	-
		Beta2 adrenoceptor	-5.399	TYR 308
		5-hydroxytryptamine receptor 2A	-3.918	LEU 209, ASP 135
		Sodium-dependent serotonin transporter	-4.272	-
		Histamine H2 receptor	-5.177	ASN 312
3	Cyanocolchicines	Muscarinic acetylcholine receptor M1	-	-
		Muscarinic acetylcholine receptor M2	-4.617	-
		Muscarinic acetylcholine receptor M3	-5.703	ILE 222, TYR 148
		Neuronal acetylcholine receptor subunit alpha-7	-	-
		D2 dopamine receptor	-	-
		Gamma-aminobutyric acid type B receptor subunit 1	-	-
		Glutamate receptor ionotropic, kainate 1	-5.009	-
		Beta2 adrenoceptor	-	-
		5-hydroxytryptamine receptor 2A	-5.806	LEU 209, ASP 135
		Sodium-dependent serotonin transporter	-6.509	ARG 104
		Histamine H2 receptor	-5.107	-
4	3Beta-methoxy-5-cholesten-19-oic acid	Muscarinic acetylcholine receptor M1	-2.903	LYS 57
		Muscarinic acetylcholine receptor M2	-3.381	ASN 404, ASP 103
		Muscarinic acetylcholine receptor M3	-7.416	ASN 507
		Neuronal acetylcholine receptor subunit alpha-7	-8.656	-
		D2 dopamine receptor	-5.911	-
		Gamma-aminobutyric acid type B receptor subunit 1	-5.911	-
		Glutamate receptor ionotropic, kainate 1	-6.572	-
		Beta2 adrenoceptor	-	-
		5-hydroxytryptamine receptor 2A	-6.860	LEU 209, ASP 135
		Sodium-dependent serotonin transporter	-6.991	TYR 175
		Histamine H2 receptor	-5.107	-
5	Cholest-5-en-3-ol (3, Beta.)-, carbonochloridate,	Muscarinic acetylcholine receptor M1	-10.159	LYS 57
		Muscarinic acetylcholine receptor M2	-5.531	-
		Muscarinic acetylcholine receptor M3	-10.788	ASP 147
		Neuronal acetylcholine receptor subunit alpha-7	-10.303	-
		D2 dopamine receptor	-6.868	ALA376
		Gamma-aminobutyric acid type B receptor subunit 1	-6.868	ALA376
		Glutamate receptor ionotropic, kainate 1	-7.117	-
		Beta2 adrenoceptor	-7.138	SER 203
		5-hydroxytryptamine receptor 2A	-7.065	LEU 209, ASP 135
		Sodium-dependent serotonin transporter	-7.696	SER 555
		Histamine H2 receptor	-6.206	-
6	Cholesterol	Muscarinic acetylcholine receptor M1	-9.955	LYS 57
		Muscarinic acetylcholine receptor M2	-4.591	-
		Muscarinic acetylcholine receptor M3	-10.534	TYR 529
		Neuronal acetylcholine receptor subunit alpha-7	-10.130	-
		D2 dopamine receptor	-6.363	-
		Gamma-aminobutyric acid type B receptor subunit 1	-6.363	-
		Glutamate receptor ionotropic, kainate 1	-7.219	-
		Beta2 adrenoceptor	-7.332	SER 203
		5-hydroxytryptamine receptor 2A	-7.280	LEU 209, ASP 135
		Sodium-dependent serotonin transporter	-7.753	SER 555
		Histamine H2 receptor	-6.044	SER 204

7	Cholest-5-en-3-ol (3, Beta.)-, propionate	Muscarinic acetylcholine receptor M1	-	-
		Muscarinic acetylcholine receptor M2	-	-
		Muscarinic acetylcholine receptor M3	-9.829	-
		Neuronal acetylcholine receptor subunit alpha-7	-9.742	-
		D2 dopamine receptor	-5.846	-
		Gamma-aminobutyric acid type B receptor subunit 1	-5.846	-
		Glutamate receptor ionotropic, kainate 1	-6.403	-
		Beta2 adrenoceptor	-	-
		5-hydroxytryptamine receptor 2A	-6.475	LEU 209, ASP 135
		Sodium-dependent serotonin transporter	-7.288	-
		Histamine H2 receptor	-6.043	TRP 313
8	Echinacoside	Muscarinic acetylcholine receptor M1	-	-
		Muscarinic acetylcholine receptor M2	-12.058	-
		Muscarinic acetylcholine receptor M3	-	-
		Neuronal acetylcholine receptor subunit alpha-7	-	-
		D2 dopamine receptor	-	-
		Gamma-aminobutyric acid type B receptor subunit 1	-	-
		Glutamate receptor ionotropic, kainate 1	-16.094	-
		Beta2 adrenoceptor	-	-
		5-hydroxytryptamine receptor 2A	-17.077	LEU 209, ASP 135
		Sodium-dependent serotonin transporter	-15.810	SER 559, GLU494, ILE552, ASP98
		Histamine H2 receptor	-17.556	SER 203, ASN 312, TYR 316, HE 93, CYS 184, ASN 103, PHE 193
Standard drugs				
1	Acetylcholine	Muscarinic acetylcholine receptor M1	-5.554	ASN 382
		Muscarinic acetylcholine receptor M2	-3.773	ASN 404, ASP 103,
		Muscarinic acetylcholine receptor M3	-6.001	-
		Neuronal acetylcholine receptor subunit alpha-7	-8.257	-
2	Dopamine	D2 dopamine receptor	-2.550	ALA376, ALA379
3	GABA	Gamma-aminobutyric acid type B receptor subunit 1	-2.182	ALA 122
4	Norepinephrine	Beta2 adrenoceptor	-8.340	SER 303, ASN 312
5	Serotonin	5-hydroxytryptamine receptor 2A	-7.848	-
		Sodium-dependent serotonin transporter	-6.190	ILE 552, GLU 494, ASP328
6	Histamine	Histamine H2 receptor	-5.393	SER 203

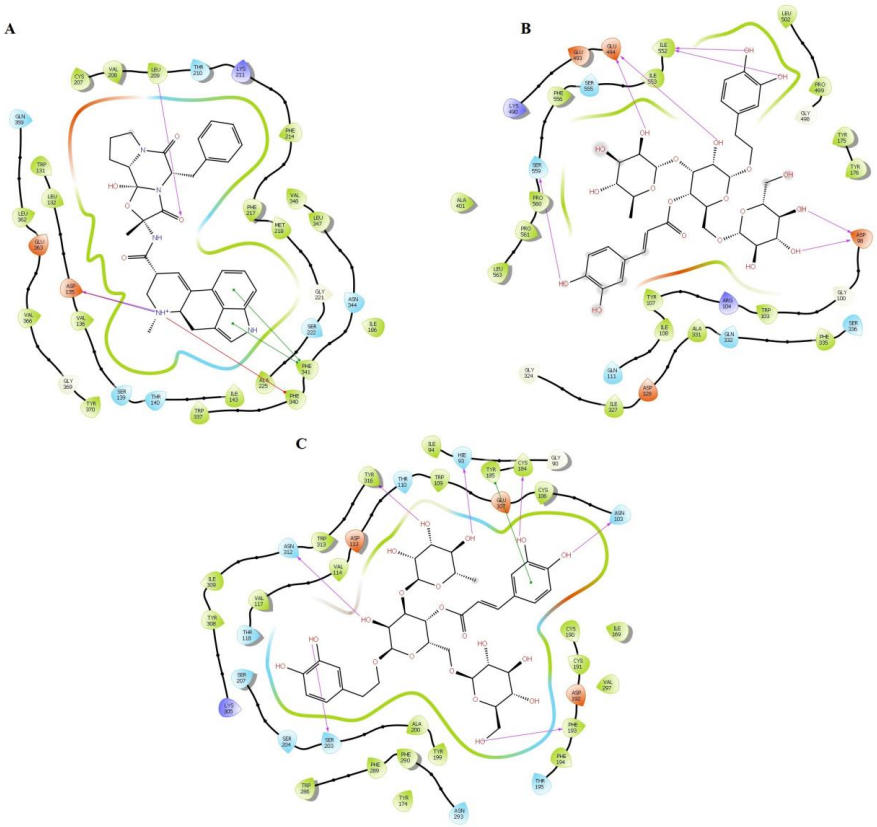

Figure 1: (A) Interaction between Echinacoside and 5-hydroxytryptamine receptor 2A (B) Interaction between Echinacoside and Sodium-dependent serotonin transporter (C) Interaction between Echinacoside and Histamine H2 receptor

Totally, eight natural compounds with six standard drugs were docked against eleven target proteins, represent as neurotransmitters. The results show among the eight natural compounds, Echinacoside has shown the highest interaction with 5-hydroxytryptamine receptor 2A, Sodium-dependent serotonin transporter, and Histamine H2 receptor. The receptors are mainly involved in neurogenic disorders in human.

Conclusion

Neurotransmitters are molecules that inhibit or stimulate a postsynaptic cell, which is released into the body by the presynaptic nerve cell to produce a response to a certain stimulus. The development of neurotransmitters and its complex functions are influenced by numerous factors. In this study, some mathematical speculations have been proposed on the basis of structural and functional characteristics of the virtual neuron (especially the physiological phenomena of human beings) with a molecular docking and biomathematical approach to formulating some speculations to the consolidation of the identification of neurotransmitters function. This could pave a way to formulate more mathematical speculations related to the neuron, and finally, these data and approaches will be useful for constructing virtual neuron with the help of biomathematics. The interaction between natural compounds and neurotransmitter studies shows the good interaction with all the compounds. Especially, 26.27-Di(nor)-cholest- 5,7,23-trien-22-ol, 3-methoxymethoxy, Cholest-5-en-3-ol (3, Beta.)-, carbonochloridate, Cholesterol and Echinacoside exhibited maximum interaction with all the target proteins. Among the other compounds, echinacoside shows highest interaction with (Serotonin) 5- hydroxytryptamine receptor 2A (-17.077), Sodium-dependent serotonin transporter (-15.810) and (Histamine) Histamine H2 receptor (-17.556).

Serotonin the other major inhibitory neurotransmitter is deemed to be the master neurotransmitter. The imbalance is one of the most often cited contributors to depression and other mood disorders. It is also intimately tied to many biological processes such as sleep, appetite, pain, digestion, and generalized well-being.

Histamine is most commonly known for its role in allergic reactions but it is also involved in neurotransmission and can affect your emotions and behavior as well. Histamine helps control the sleep-wake cycle and promotes the release of epinephrine and norepinephrine.

Serotonin and histamine were the brain monoamines which play a vital role in cognition, emotions, pathophysiology, and treatment of mental disorders. In the current study revealed that the neurotransmitters structure and transportation by mathematical models and in silico molecular docking results strongly shows the Echinacoside is a potent inhibitor in some neurological disorder associated with serotonin and histamine. Further, extend methods adapt to study the mechanism and pathway level interactions between the natural compounds with the disease .

Conflict of Interest

We have no conflict of interests to disclose and the manuscript has been read and approved by all named authors.

Acknowledgement

This work was supported by the Philosophical and Social Sciences Research Project of Hubei Education Department (19Y049), and the Staring Research Foundation for the Ph.D. of Hubei University of Technology (BSQD2019054), Hubei Province, China.

Reference

1. Hyman, S. E. (2005). Neurotransmitters. Current biology, 15(5), R154-R158.
2. Masland, R. H. (2004). Neuronal cell types. Current Biology, 14(13), R497-R500.
3. Nestler, E. J., Hyman, S. E., & Malenka, R. C. (2001). Molecular neuropharmacology: a foundation for clinical neuroscience. McGraw-Hill Medical.
4. Pestana, M., Jardim, H., Correia, F., Vieira-Coelho, M. A., & Soares-da-Silva, P. (2001). Renal dopaminergic mechanisms in renal parenchymal diseases and hypertension. Nephrology Dialysis Transplantation, 16(suppl_1), 53-59.
5. Marko, A. M., Gerrard, J. W., & Buchan, D. J. (1960). Glutamic Acid Derivatives in Adult Celiac Disease: II. Urinary Total Glutamic Acid Excretion. Canadian Medical Association Journal, 83(25), 1324.
6. Bélanger, R., Chandramohan, N., Misbin, R., & Rivlin, R. S. (1972). Tyrosine and glutamic acid in plasma and urine of patients with altered thyroid function. Metabolism, 21(9), 855-865.
7. Ragginer, C., Lechner, A., Bernecker, C., Horejsi, R., Möller, R., Wallner-Blazek, M., ... & Gruber, H. J. (2012). Reduced urinary glutamate levels are associated with the frequency of migraine attacks in females. European Journal of Neurology, 19(8), 1146-1150.
8. Field, T., Diego, M., Hernandez-Reif, M., Figueiredo, B., Deeds, O., Ascencio, A., ... & Kuhn, C. (2010). Comorbid depression and anxiety effects on pregnancy and neonatal outcome. Infant Behavior and Development, 33(1), 23-29.
9. Ghaddar, A., Omar, K. H., Dokmak, M., Abou Kansour, N., Jbara, Z., Laham, S., & Ali, S. (2013). Work-related stress and urinary catecholamines among laboratory technicians. Journal of occupational health, 55(5), 398-404.
10. Liu, L., Li, Q., Li, N., Ling, J., Liu, R., Wang, Y., ... & Bi, K. (2011). Simultaneous determination of catecholamines and their metabolites related to Alzheimer's disease in human urine. Journal of separation science, 34(10), 1198-1204.
11. Paine, N. J., Watkins, L. L., Blumenthal, J. A., Kuhn, C. M., & Sherwood, A. (2015). Associations of Depressive and Anxiety Symptoms with 24-hour Urinary Catecholamines in individuals with untreated high blood pressure. Psychosomatic medicine, 77(2), 136.\
12. Hughes, J. W., Watkins, L., Blumenthal, J. A., Kuhn, C., & Sherwood, A. (2004). Depression and anxiety symptoms are related to increased 24-hour urinary norepinephrine excretion among healthy middle-aged women. Journal of psychosomatic research, 57(4), 353-358.
13. Koslow, S. H., Maas, J. W., Bowden, C. L., Davis, J. M., Hanin, I., & Javaid, J. (1983). CSF and urinary biogenic amines and metabolites in depression and mania: A controlled, univariate analysis. Archives of general psychiatry, 40(9), 999-1010.
14. Nicholson-Guthrie, C. S., Guthrie, G. D., Sutton, G. P., & Baenziger, J. C. (2001). Urine GABA levels in ovarian cancer patients:: elevated GABA in malignancy. Cancer letters, 162(1), 27-30.
15. Nichkova, M. I., Huisman, H., Wynveen, P. M., Marc, D. T., Olson, K. L., & Kellermann, G. H. (2012). Evaluation of a novel ELISA for serotonin: urinary serotonin as a potential biomarker for depression. Analytical and bioanalytical chemistry, 402(4), 1593-1600.
16. Aruoma, O. I., Bahorun, T., & Jen, L. S. (2003). Neuroprotection by bioactive components in medicinal and food plant extracts. Mutation Research/Reviews in Mutation Research, 544(2-3), 203-215.
17. Zhao, B., Diraviyam, T., & Zhang, X. (2015). A bio-mathematical approach: Speculations to construct virtual placenta. Applied Mathematics and Computation, 256, 344-351.
18. Cumpson, P., & Sano, N. (2012). Stability of reference masses V: UV/ozone treatment of gold and platinum surfaces. Metrologia, 50(1), 27.
19. S. Ganesh, J. Jannet Vennila, A. Annie Mercy, Effects of Phytochemicals extracted from Acanthus Ilicifolius against Staphylococcus aureus: An In-silico approach, American Journal of Drug Discovery and Development.3 (4) (2013) 293-297.
20. Wang, T., Zhang, X., & Xie, W. (2012). Cistanche deserticola YC Ma," Desert ginseng": a review. The American Journal of Chinese Medicine, 40(06), 1123-1141.
21. Meraj, K., Mahto, M. K., Christina, N. B., Desai, N., Shahbazi, S., & Bhaskar, M. (2012). Molecular modeling, docking and ADMET studies towards development of novel Disopyramide analogs for potential inhibition of human voltage gated sodium channel proteins. Bioinformation, 8(23), 1139.
22. Egan, W. J. (2007). Computational models for ADME. Annual reports in medicinal chemistry, 42, 449-467.
23. H. Pollard, J. C. Schwartz, Trends Neurosci. 10,86-89. 1987
24. J. T. Schmidt, Proc. R. Soc. London Ser. B 205, (1979) 287-306.
25. J. T. Schmidt, J. A. Freeman, Brain Res. 187, (1980) 129-142.
26. P. G. Strange, In Dopamine Receptors (Fraser, C. M. & Creese, I., eds.), A. R. Liss, New York. 1987.
27. Asano, T., Ui, M., & Ogasawara, N. (1985). Prevention of the agonist binding to gamma-aminobutyric acid B receptors by guanine nucleotides and islet-activating protein, pertussis toxin, in bovine cerebral cortex. Possible coupling of the toxin-sensitive GTP-binding proteins to receptors. Journal of Biological Chemistry, 260(23), 12653-12658.
28. D. T. Monaghan, C. W. Cotman, Proc. Natl. Acad.Sci. U.S.A. 83, (1986) 7533-7536.
29. F. E. Bloom, The Neurosciences, Fourth Study Program (Schmitt, F. 0. & Worden, F. G., eds.), pp. 51-58, MITPress, Cambridge, MA. 1979.
30. Okoh, D., Owolabi, O., Ekechukwu, C., Folarin, O., Arhiwo, G., Agbo, J., ... & Rabiu, B. (2016). A regional GNSS-VTEC model over Nigeria using neural networks: A novel approach. Geodesy and Geodynamics, 7(1), 19-31.
31. Shen, J., Tan, C., Zhang, Y., Li, X., Li, W., Huang, J., ... &

Tang, Y. (2010). Discovery of potent ligands for estrogen receptor β by structure-based virtual screening. Journal of medicinal chemistry, 53(14), 5361-5365.
32. Li, X. L., & Wei, J. J. (2013). Stability and bifurcation analysis in a system of four coupled neurons with multiple delays. Acta Mathematicae Applicatae Sinica, English Series, 29(2), 425-447.
33. Chen, S., Zhang, X. J., Li, L. X., Wang, Y., Zhong, R. J., & Le, W. (2015). Histone deacetylase 6 delays motor neuron degeneration by ameliorating the autophagic flux defect in a transgenic mouse model of amyotrophic lateral sclerosis. Neuroscience bulletin, 31(4), 459-468.
34. Urbanska, M., Blazejczyk, M., & Jaworski, J. (2008). Molecular basis of dendritic arborization. Acta neurobiologiae experimentalis, 68(2), 264.
35. Yousefi, F., & Amoozandeh, Z. (2016). Statistical mechanics and artificial intelligence to model the thermodynamic properties of pure and mixture of ionic liquids. Chinese Journal of Chemical Engineering, 24(12), 1761-1771.
36. Yousefi, F., & Amoozandeh, Z. (2017). A new model to predict the densities of nanofluids using statistical mechanics and artificial intelligent plus principal component analysis. Chinese journal of chemical engineering, 25(9), 1273-1281.
37. Xie, Y., Kang, Y., Liu, Y., & Wu, Y. (2014). Firing properties and synchronization rate in fractional-order Hindmarsh-Rose model neurons. Science China Technological Sciences, 57(5), 914-922.
38. Zhao, J., Xu, H., Tian, Y., Hu, M., & Xiao, H. (2013). Effect of electroacupuncture on brain-derived neurotrophic factor mRNA expression in mouse hippocampus following cerebral ischemia-reperfusion injury. Journal of Traditional Chinese Medicine, 33(2), 253-257.
39. CUI, H. Y., Chen, F. E. N. G., & LIU, Y. J. (2013). Analysis of prediction performance in wavelet minimum complexity echo state network. The Journal of China Universities of Posts and Telecommunications, 20(4), 59-66.
40. J. L. Barker, R. M. McBurney, Proc. R. Soc. London Ser. B 206 1979: 319-327.
41. Kosofsky, B. E., Molliver, M. E., Morrison, J. H., & Foote, S. L. (1984). The serotonin and norepinephrine innervation of primary visual cortex in the cynomolgus monkey (Macaca fascicularis). Journal of Comparative Neurology, 230(2), 168-178.
42. Brown, D. (1986). Neuropharmacology: Acetylcholine and brain cells. Nature, 319(6052), 358-359.
43. J. R. Brow (1983) Arbuthnott Neuroscience 10: 349-355.
44. R. Y. Moore, F. E. Bloom, Annu. Rev. Neurosci. 2, 113-168. 1979
45. C. W. Cotman, L. L. Iversen, Trends Neurosci. 10, 263-265. 1987
46. Shen, J., Tan, C., Zhang, Y., Li, X., Li, W., Huang, J., ... & Tang, Y. (2010). Discovery of potent ligands for estrogen receptor β by structure-based virtual screening. Journal of medicinal chemistry, 53(14), 5361-5365.
47. César-Razquin, A., Snijder, B., Frappier-Brinton, T., Isserlin, R., Gyimesi, G., Bai, X., ... & Superti-Furga, G. (2015). A call for systematic research on solute carriers. Cell, 162(3), 478-487.
48. Chambers, J. K., Macdonald, L. E., Sarau, H. M., Ames, R. S., Freeman, K., Foley, J. J., ... & Livi, G. P. (2000). AG protein-coupled receptor for UDP-glucose. Journal of Biological Chemistry, 275(15), 10767-10771.